Pergamon
www.elsevier.com/locate/asr

Adv. Space Res. Vol. 27, Nos 6–7, pp. 1181–1187, 2001

Printed in Great Britain
0273-1177/01 $20.00 + 0.00
PII: S0273-1177(01)00164-8

MONITORING THE MOON'S TRANSIENT ATMOSPHERE WITH AN ALL-SKY IMAGER

S.M. Smith, M. Mendillo, J.K. Wilson and J. Baumgardner

Center for Space Physics, Boston University, 725 Commonwealth Ave, Boston, MA 02215, USA

ABSTRACT

An indispensable tool in terrestrial aeronomy, all-sky imaging has recently been shown to be useful in studies of the Moon's exosphere. Two days after the peak of the 1998 Leonid meteor shower, an extended region of neutral sodium emission was detected in the night sky using a bare-CCD imaging system. The feature was found to be a train of sodium gas originating from the Moon. Subsequent observations indicate the feature is normally visible (max. brightness ~15-90 Rayleighs (R)) during nights near the time of new Moon. Monthly monitoring of the feature using an all-sky system can provide useful information about the time-variability of the lunar atmosphere. Several processes are believed to be responsible for the production of lunar Na and evidence is presented indicating that two of these processes were each responsible for the observed brightness enhancements of the sodium feature on two separate new Moon periods in January and March 2000.

INTRODUCTION

All-sky imagers have been used for many years to monitor terrestrial phenomena such as mesospheric gravity waves (e.g., Taylor *et al.*, 1995; Swenson *et al.*, 1995; Smith *et al.*, 2000), equatorial airglow depletions (e.g., Mendillo *et al.*, 1997; Taylor *et al.*, 1997), and aurorae (Eather, 1984; Weber *et al.*, 1984; Steele and Cooger, 1996). This paper describes a new and novel use for all-sky imaging, namely, the routine monitoring of the transient lunar atmosphere (Smith *et al.*, 1999). Observations are made around the time of new Moon when, paradoxically, the Moon is not present in the sky. The observations can be made easily during simultaneous imaging of the Na airglow in the terrestrial mesosphere.

A comprehensive review of the lunar atmosphere and the processes responsible for its production was made by Stern (1999). The main processes are (1) Photon sputtering: also called photon-stimulated desorption, this process involves the liberation of Na atoms from the lunar surface by direct photon energy transfer. (2) Ion sputtering: direct impact of surface Na by charged solar wind particles such as protons, electrons and ionized He. (3) Chemical sputtering: this process involves the liberation of lunar Na by obtaining excess energy through a chemical reaction with the solar wind particles on the surface as opposed to direct ion impact. (4) Thermal desorption: evaporation of material from the surface. (5) Meteoric impact vaporization: the liberation of Na by the impact of the meteoric material onto the lunar surface causing vaporization of the upper layer of the lunar regolith and the incident meteoroid. Processes (1-4) create an Na source which varies with solar zenith angle and has a maximum at the sub-solar point. A regular sporadic micro-meteor source is assumed to be spherically uniform and so does not exhibit a zenith angle effect. Routine monthly all-sky observations of the feature, especially during periods of increased solar and meteor shower activity, will be extremely useful because the relative importance of each process listed above is still uncertain.

INSTRUMENTS AND PREVIOUS OBSERVATIONS

The all-sky imaging system used in this study has been described previously (Baumgardner *et al.*, 1993; Smith *et al.*, 2000); briefly, the detector consists of a cooled (-40°C) 1024 x 1024-pixel bare charge-coupled device (CCD) with a dark count of ~1 electrons pixel^{-1} s^{-1} and a read-out noise level of 6 electrons pixel^{-1}. The system is used to routinely image gravity wave activity in the mesospheric hydroxyl (OH Meinel bands in the near-infrared (NIR) (695 ~ 950 nm)), neutral sodium (589.1 nm, FWHM = 1.9 nm) and atomic oxygen (557.7 nm, FWHM = 1.2 nm) layers near 87, 90 and 96 km, respectively (Smith *et al.*, 2000). Observations are typically made on the 14 nights centered on the time of new Moon. The typical integration time used for the Na emission and off-band images is 120 s. An off-band image at 644.4 nm (FWHM = 1.4 nm) is acquired every 30 minutes.

The all-sky observations were made at Millstone Hill (42°36'N, 7°30'W) and periodically at the Boston University Station at McDonald Observatory, Fort Davis, Texas (30° 49'N, 104° 01'W). The feature was first observed during the new Moon period in November 1998 (Smith *et al.*, 1999), two nights after the peak of the Leonid meteor shower. The top-left panel of Figure 1 shows an example of a raw image of the emission feature (spot) taken on 19 November 1998 UT. To the right is a magnified view of the feature, time-averaged over the night. Generally, the size of the spot at new Moon is approximately 3° x 3° (FWHM).

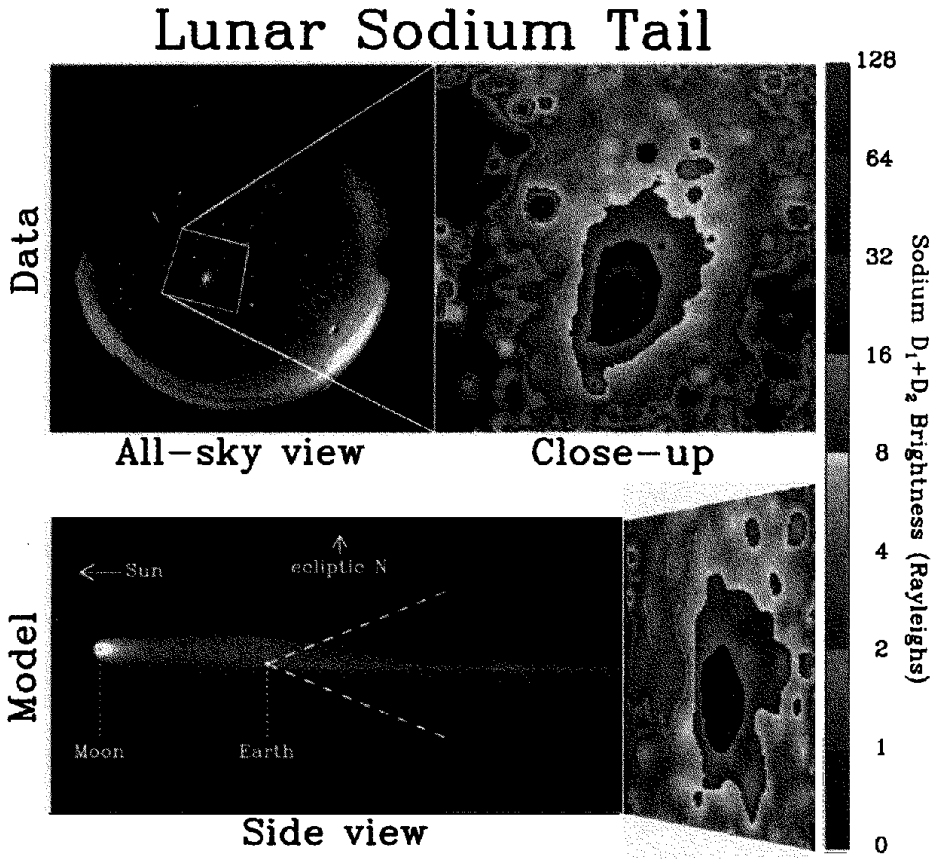

Figure 1: Top-left Panel: Raw discovery all-sky image of the sodium emission feature on 19 November 1998. Top-right Panel: Magnified false-color image of the feature, time-averaged over the night of 19 November 1998. Bottom-left Panel: Computer-model of Earth-Moon system at new Moon on 19 November 1998 04:27 UT showing (to scale) neutral sodium tail originating from Moon and extending anti-sunward past the Earth. A small amount of gravitational focussing by the Earth occurs as the Na streams past and this can be seen here as an enhancement in the tail brightness extending anti-sunward from behind the Earth. The all-sky camera field of view from the Earth is indicated by the dotted lines. Bottom-right Panel: Model view of the tail as seen from Earth (viewed obliquely).

The feature was shown to undergo similar nightly brightness and morphology variations during the two new Moon periods in August and November 1998 (Smith *et al.*, 1999). On the night prior to new Moon, the feature exhibited a faint streak-like shape of approximately 5° in length. On the night closest to new Moon, the feature was brighter, larger and more elliptically-shaped. On the following night, the feature had decreased in brightness and had regained its original streak-like shape, but which was now oriented approximately 90° to the first night's apparition. We attributed the feature to an extended trail of neutral Na gas of lunar origin. The lunar Na is blown anti-sunward into a tail by solar radiation pressure and the Na glows due to resonance scattering by sunlight. The lower-left panel in Figure 1 is a computer-modeled image of the Earth-Moon system and the sodium tail as viewed from the side. A slight "focussing" of the Na atoms by the Earth's gravity occurs as they stream past the Earth. This focussing (clearly seen in this model image) results in a slight enhancement in the brightness of the sodium tail behind the Earth. To the right is a computer-modeled view of the tail as seen from Earth (viewed obliquely). The brightness and morphology of the feature in this view is remarkably similar that seen in the all-sky images.

Monte-Carlo numerical modeling (Wilson *et al.*, 1999) has shown that the tail is present continuously but is only visible from the Earth during 2-3 nights centered on the new Moon. In addition, the brightness and morphology of the feature was shown to vary according to the amount of Na in the tail and the relative positions of Earth and Moon. If the rate of Na production is constant with time, the feature will appear to be brightest on the night closest to new Moon. At the time of new Moon, the tail extends directly away from the Earth and integrated emission along the length of the tail allows the feature to be visible. The modeling also indicated that the spot's maximum brightness was reduced by <20% by the Earth's umbra.

Because no major meteor shower activity occurred within 10 days prior to the August 1998 new moon we attributed 3-4-fold brightness enhancement observed in November 1998 (90±5 R), compared to August 1998 (19±6 R), to an increased lunar Na production rate by the Leonid meteor shower which peaked two days prior to the new Moon. The brightness enhancement was the clearest evidence to date of a meteoric effect on the lunar atmosphere.

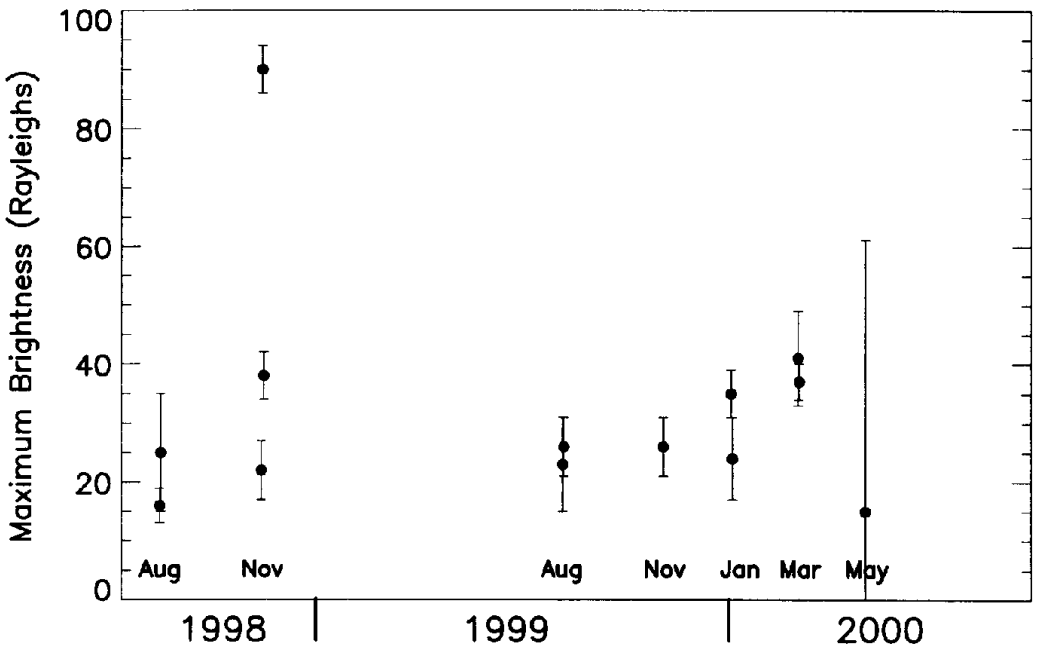

Figure 2: Brightness variations of the lunar sodium tail feature during the period August 1998 to May 2000. The observations from August 1998 to November 1999 were made at McDonald Observatory, TX. The observations in 2000 were made at Millstone Hill, MA. There is considerable variability in the feature's brightness from month to month. This is interpreted as variations of the precursory processes responsible for the production of lunar Na.

RESULTS AND DISCUSSION

Observations at the McDonald Observatory site are made only infrequently, usually in the summer and fall months, but the feature has been detected from there during every observed new Moon period. At Millstone Hill, the spot has not been detected during every new Moon period because anthropogenic sodium emission from the city of Boston and environs prevents detection of the faint spot there, especially when it is low on the horizon. Adverse weather and technical problems also prevented its detection during some months.

The spot has now been detected during seven new Moon periods since August 1998 and its maximum brightness ranged from 15 to 90 R. Figure 2 shows the observed brightness of the Na feature during several new Moon periods between the August 1998 and May 2000. The feature is clearly variable in brightness from month to month. The first two detections (made at McDonald Observatory) show clearly the 3-4-fold brightness enhancement of the feature in November 1998 compared to August 1998. Observations at Millstone Hill (the last three detections) showed evidence of brightness enhancements resulting from the Quadrantid meteor shower in January 2000 (meteoric impact vaporization), and due to increased solar UV radiation in March 2000 (photon desorption source). These particular months' observations will be discussed later in detail. The May 2000 measurement resulted from only one image during the night of 4 May 2000 because of clouds. The levels of solar and meteor activity during each new Moon period were examined in relation to the month-to-month brightness variations of the spot in order to ascertain the relative importance of the Na production proceses mentioned earlier.

Table 1 lists the levels of the solar radio flux at $\lambda = 10.7$ cm (F10.7 flux) (a proxy for the level of solar UV activity) and the solar wind density and speed, as well as the observation time and brightness of the feature for five of the months shown in Figure 2. The observation times relative to the time of new Moon (ΔT) are also listed because the brightness and morphology of the feature are both markedly dependent on the time of new Moon. The solar wind and F10.7 cm flux values listed in Table 1, and used in this paper, are the mean values which occurred at 48±3 hours prior to the new Moon spot observations because it takes ~2 days for the Na atoms from the lunar surface to reach the vicinity of the Earth (Wilson *et al.*, 1999).

Table 1. The lunar sodium tail emission brightness on nights closest to new Moon for selected months together with the mean solar wind and F10.7cm flux values for the period 48±3 hours prior to the midpoint of each observation period. The parameter ΔT is the difference, in hours, between the time of new Moon and the mid-time of the observation period.

Date	Spot Brightness (Rayleighs)	ΔT (hours)	Solar Wind Density (cm^{-3})	Solar Wind Speed ($km\ s^{-1}$)	Solar F10.7 cm Flux (10^{22} J s^{-1} m^{-2} Hz^{-1})
22 Aug 1998	25±10	+2.71	16.8±7.9	312±16	137.1±3.5
19 Nov 1999	90±4	+2.33	6.2±0.3	451±23	123.9±3.2
11 Aug 1999	23±8	-5.93	10.0±4.9	387±6	139.0±1.7
7 Jan 2000	35±4	+12.59	3.2±0.1	524±13	135.6±1.3
6 Mar 2000	41±8	+0.03	0-2	320	202.7±1.6

Observations made at similar seasons separated by a year provides an interesting test for the relative importance of the source processes of lunar Na production. However, because the lunar phase is not fixed to the sidereal calendar (new Moon fell on August 22 in 1998 and August 11 in 1999) one needs to note the time of new Moon when making lunar spot comparisons that are separated by one year. For example, observations made of the spot were obtained during August 1998 and August 1999. The spot reached a maximum brightness of 25±10 R (August 1998) and 26±5 R (August 1999). No major meteor shower activity occurred within one week prior to the August 1998 new Moon. The 1999 Perseid meteor shower peaked at August $12^{d}23^{h}08^{m}$ UT (McBeath, 1998), 35 hours after time of the August new Moon ($11^{d}11^{h}08^{m}$ UT). The full-width at half maximum of the shower peak was approximately 6 hours and the last night of observations were made nearly 13 hours before the time of the shower maximum, so the level of meteor activity could be considered to be around sporadic levels, similar to those encountered during August 1998. The F10.7 flux values, and hence the level of solar UV radiation (photon desorption source), prior to the August 1998 and 1999 new Moon observations were similar, being 137.1±3.5 (±σ) and 139.0±1.7 W m^{-2}, respectively (Table 1). The solar wind activities (ion-sputtering source) prior to new Moon in August 1998 and August 1999 were also at similar levels. The solar wind speed was approximately 19% higher in August 1999 (387±6 km s^{-1}) compared to in August 1998 (312±16 km s^{-1}) (Table 1). This increase corresponds to the solar wind particles, on average, possessing approximately 54% greater kinetic energy to impart to the lunar

surface. The solar wind density was, however, 40% lower in August 1999 (10.0±4.9 cm^{-3}) than in August 1998 (16.8±7.9 cm^{-3}), so the solar wind did not appear to have a significant effect on the brightness of the feature. From this comparison, the brightness of the spot in August 1998 and August 1999 is due to relatively similar levels of solar and meteor activity and, as such, can be used as a benchmark for comparison with other months.

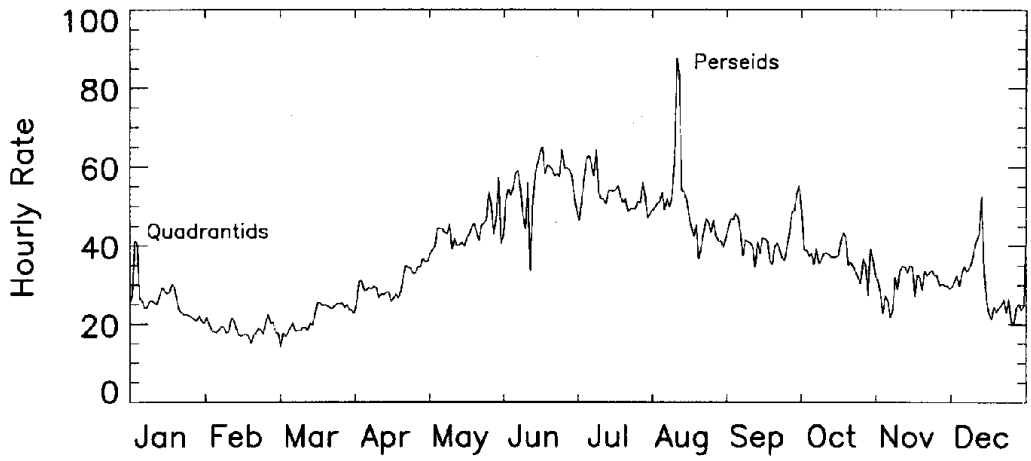

Figure 3: Daily hourly-rate of terrestrial meteor activity as a function of season for the years 1989 to 1994 as measured by the Sheffield Meteor Radar. There is a clear annual variation in meteor activity interspersed with sharp peaks due to meteor showers, such as the Quadrantids (Jan 6) and the Perseids (Aug 12). Data supplied courtesy of V.S. Howells and H.R. Middleton, MLT Dynamics Group, University of Wales, Aberystwyth.

The brightness of the feature during the January 2000 new Moon period was larger (35±4 R) compared to the August 1998 and August 1999 apparitions. In an analogous way to November 1998, the peak of the 2000 Quadrantid meteor shower occurred approximately 2 days before the time of new Moon (Jan 6 11:45 UT) on Jan 4 at 05:00 UT (McBeath and Arlt, 1999). The values in Table 1 indicate that the F10.7 cm flux was similar to that observed in August 1998 and August 1999. The solar wind density and speed prior to the January observations were 3.2±0.1 cm^{-3} and 524±13 km s^{-1}, respectively (Table 1). The solar wind speed was higher by 50% (a factor of ~1.5) than observed during August 1998 and August 1999. Although this corresponded to a more than two-fold increase in the average particle energy, the solar wind density was 76% lower. The 7 January 2000 observations were made over 12 hours after new Moon but the feature is nearly 23% brighter than during the meteor shower-free periods in August 1998 and 1999. Of particular note, the brightness of the feature on the 8 January, over 33 hours after new Moon, was comparable with the brightness of the feature observed within several hours of new Moon, such as 22 August 1998 and 11 August, 1999. We attribute the brightness enhancement in January 2000 to be due, in part at least, to an enhancement in lunar Na production as a result of increased meteor lunar impacts by the Quadrantid meteor shower.

The other month of interest was during the new Moon period of March 6, 2000. At that time, the feature attained a maximum brightness of 41±8 R. The 10.7 cm solar flux prior to the observations was 202.7±1.6 W m^{-2} (Table 1); a 47% increase compared to the August 1998 and August 1999 periods. However, the solar wind activity was lower than during any other time. The solar wind density was 0-2 cm^{-3} and the solar wind speed was ~320 km s^{-1}. Like the August 1998 lunation, there was no major meteor shower activity prior to the March 2000 lunation. Furthermore, time-averaged data from the Sheffield Meteor radar for the years 1989-1994 (Figure 3) indicated that the seasonal meteor count in early March is usually less than half that occurring in the month of August. These results suggest that the ~1.5-times greater solar UV flux prior to the March 2000 new Moon period was responsible for the 1.6-times enhancement in the feature's brightness in March 2000 compared to that seen in August 1998 and 1999. We conclude that during this period, photon desorption was the dominant process as a source of high speed Na in the lunar atmosphere (Sprague *et al.*, 1992, 1998).

There is little doubt that there is a significant solar influence on the variability of the lunar atmosphere. Mendillo *et al.*, (1991), found evidence of a zenith angle effect in the distribution on Na. Further imaging studies of the Moon during several lunar eclipses were made by Mendillo *et al.*, (1999). During such periods the Moon resides in the terrestrial magnetotail and so is assumed to be shielded from a solar wind sputtering source. The study by Mendillo *et al.*, (1999) also found no reduction in the Na distribution, and suggested that photon desorption (Sprague *et al.*, 1992), as opposed to sputtering from solar wind particles, was a more important process for the production of lunar Na. This issue of solar wind sputtering's role as an important source mechanism was also addressed by Potter and Morgan (1991, 1994). In their most recent study, Potter and Morgan (2000) suggest that solar photon desorption (sputtering) is the dominant source of exospheric Na but that solar wind particles are also involved by bringing Na to the lunar surface where it is ejected into the exosphere by photon desorption.

SUMMARY

An emission feature with a brightness ranging from 15 to 90 R and approximately 3^{o} x 3^{o} in extent has been observed to occur near the anti-solar/lunar points 2 to 3 days around the time of new Moon (Smith *et al.*, 1999). The feature shines only at 589 nm and is attributed to a long train of neutral sodium gas originating from the lunar surface. The tail is apparently present all the time but is only visible from the Earth during the new Moon period because of its extreme faintness. The emission feature has been detected during seven new Moon periods since its first detection in November 1998 and its maximum brightness varies from month to month, suggesting that the sources responsible for its production are also variable. Evidence suggests that the brightness enhancements of the feature during the new Moon periods of January 2000 and March 2000 were due to meteoric impact vaporization and, for the first time, to increased solar photon desorption from the lunar surface, respectively. To confirm that transient photon effects play a role in lunar atmosphere variability, more observations are clearly needed.

All-sky imaging provides a simple method for the long-term monitoring of the Moon's transient atmosphere. No tracking is required and there is no scattered moonlight to contend with. Long-term monitoring will provide a useful test for the relative importance of the source processes responsible for the production of the moon's transient atmosphere.

There is a need to coordinate measurements made by imaging groups around the globe. Observations made at more than one particular geographic location would allow longer continuous imaging of the spot spanning a time longer than a single night during the new Moon period. For example, Shiokawa *et al.*, (2000) combined observations made in Japan with the results of Smith *et al.*, (1999) to further refine the time history of the spot brightness following the 1998 Leonid meteor shower. Also, the effects of adverse weather can be minimized by geographically-spaced observations. A coordinated observing program known as the Sodium Tail Optical Monitoring Program (STOMP) has been initiated. Interested groups and individuals are invited to participate in this study. Further information can be obtained by emailing Dr. Steve Smith at smsm@bu.edu.

ACKNOWLEDGEMENTS

The authors would like to thank the COSPAR committee for providing valuable travel assistance to present this paper at the COSPAR 2000 Meeting in Warsaw in July 2000. The authors would also like to thank the director and staff at the Millstone Hill Observatory and the McDonald Observatory for continued support for their activities there. The authors are very grateful to V.S. Howell and H. Middleton at MLT Dynamics Group, University of Wales, Aberystwyth, for providing the meteor radar data. This work was supported, in part, by grants from the NASA Planetary Astronomy program, the NSF Aeronomy program and seed funds from the Center for Space Physics at Boston University.

REFERENCES

Baumgardner, J., B. Flynn, and M. Mendillo, Monochromatic imaging instrumentation for application in aeronomy of the Earth and planets, *Opt. Eng.*, **32**, 3028-3032, 1993.

Eather, R.H., Dayside Auroral Dynamics, *Journ. Geophys. Res.*, **89**, 1695-1700, 1984.

McBeath, A., International Meteor Organization; http://www.imo.net/calendar/cal99.html, 1998.

McBeath, A. and R. Arlt, International Meteor Organization; http://www.imo.net/calendar/cal00.html, 1999.

Mendillo, M., B. Flynn, and J. Baumgardner, Imaging experiments to detect an extended sodium atmosphere on the Moon, *Geophys. Res. Lett.*, **18**, 2097-2100, 1991.

Mendillo, M., J. Baumgardner, D. Nottingham, J. Aarons, B. Reinisch, J. Scali and M. Kelley, Investigations of the thermospheric-ionospheric dynamics with 6300-Å images from the Arecibo Observatory, *Journ. Geophys. Res.*, **102**, 7331-7343, 1997.

Mendillo, M., J. Baumgardner and J. Wilson, Observational Test for the Solar Wind Origin of the Moon's Extended Sodium Atmosphere, *Icarus*, **137,** 13-23, 1999.

Potter, A.E. and T.H. Morgan, Observations of the Lunar Sodium Exosphere, *Geophys. Res. Lett.*, **18**, 2089-2092, 1991.

Potter, A.E. and T.H. Morgan, Variation of Lunar Sodium Emission Intensity with Phase Angle, *Geophys. Res. Lett.*, **21**, 2263-2266, 1994.

Potter, A.E., R.M. Killen, and T.H. Morgan, Variation of lunar sodium during the passage of the Moon through the Earth's magnetotail, *Journ. Geophys. Res.*, **105**, 15073-15084, 2000.

Shiokawa, K., M.K. Ejiri, T. Ogawa, and T. Nakamura, Distant lunar sodium tail observed in the Japanese local-time sector during the Leonid meteor shower of 1998, Journ. Geophys. Res., in press, 2000.

Smith, S.M., J.K. Wilson, J. Baumgardner, and M. Mendillo, Discovery of the Distant Sodium Tail and its Enhancement Following the Leonid Meteor Shower, *Geophys. Res. Lett.*, **26**, 1649-1652, 1999.

Smith, S.M., M. Mendillo, J. Baumgardner, and R.R. Clark, Gravity Wave Activity at a Sub-auroral Site: First Results From Millstone Hill, *Journ. Geophys. Res.*, in press, 2000.

Sprague, A.L., R.W.H. Kozlowski, D.M. Hunten, W.K. Wells, and F.A. Grosse, The Sodium and Potassium Atmosphere of the Moon and Its Interaction with the Surface, *Icarus*, **96**, 27-42, 1992.

Sprague, A.L., D.M. Hunten, R.W.H. Kozlowski, F.A. Grosse, R.E. Hill, and R.L. Morris, Observations of Sodium in the Lunar Atmosphere During International Lunar Atmosphere Week 1995, *Icarus*, **131**, 372-381, 1998.

Steele, D.P and L.L. Cogger, Polar patches and the "tongue of ionization", *Rad. Sci.*, **31**, 667-677, 1996.

Stern, S.A., The Lunar Atmosphere: History, Status, Current Problems, and Context, *Rev. Geophys.*, **37**, 453-491, 1999.

Swenson, G.R., M.J. Taylor, P.J. Espy, C. Gardner, and X. Tac, ALOHA-93 measurements of intrinsic AGW characteristics using airborne imager and groundbased Na Wind/Temperature lidar, *Geophys. Res. Lett.*, **22**, 2841-2844, 1995.

Taylor, M.J., J.V. Eccles, J. LaBelle, and J.H.A. Sobral, High resolution OI (630 nm) image measurements of F-region depletion drifts during the Guara campaign, *Geophys. Res. Lett.*, **24**, 1699-1702, 1997.

Taylor, M.J., M.B. Bishop, and V. Taylor, All-sky measurements of short period waves imaged in the OI(557.7 nm), Na(589.2 nm) and near-infrared OH and $O_2(0,1)$ nightglow emissions during the ALOHA-93 campaign, *Geophys. Res. Lett.*, **24**, 2833-2836, 1995.

Weber, E.J., J. Buchau, J.G. Moore, J.R. Sharber, R.C. Livingston, J.D. Winningham, and B.W. Reinisch, F Layer Ionization Patches in the Polar Cap, *Journ. Geophys. Res.*, **89**, 1683-1694, 1984.

Wilson, J.K., S.M. Smith, J. Baumgardner, J., and M. Mendillo, Modeling an Enhancement of the Leonid Meteor Shower During the Leonid Meteor Shower of 1998, *Geophys. Res. Lett.*, **26**, 1645-1648, 1999.